

## Pyrolytic Decomposition of Ammonia Borane to Boron Nitride

Samuel Frueh,<sup>†</sup> Richard Kellett,<sup>‡</sup> Carl Mallery,<sup>‡</sup> Trent Molter,<sup>§</sup> William S. Willis,<sup>†</sup> Cecil King'ondu,<sup>†</sup> and Steven L. Suib<sup>\*†,||,⊥</sup>

<sup>†</sup>Unit 3060, Department of Chemistry, University of Connecticut, Storrs, Connecticut 06269-3060, United States, <sup>‡</sup>Ensign Bickford Aerospace and Defense Company, 640 Hopmeadow Street, P.O. Box 429 Simsbury, Connecticut 06070-042, <sup>§</sup>Connecticut Global Fuel Cell Center, University of Connecticut, 44 Weaver Road, Unit 5233, Storrs, Connecticut 06269-5233, United States, <sup>||</sup>Department of Chemical Engineering, University of Connecticut, Storrs, Connecticut 06269, United States, and <sup>⊥</sup>Institute of Materials Science, University of Connecticut, Storrs, Connecticut 06269, United States

Received May 20, 2010

The thermal decomposition of ammonia borane was studied using a variety of methods to qualitatively identify gas and remnant solid phase species after thermal treatments up to 1500 °C. At about 110 °C, ammonia borane begins to decompose yielding H<sub>2</sub> as the major gas phase product. A two step decomposition process leading to a polymeric  $-\text{[NH=BH]}_n-$  species above 130 °C is generally accepted. In this comprehensive study of decomposition pathways, we confirm the first two decomposition steps and identify a third process initiating at 1170 °C which leads to a semicrystalline hexagonal phase boron nitride. Thermogravimetric analysis (TGA) was used to identify the onset of the third step. Temperature programmed desorption-mass spectroscopy (TPD-MS) and vacuum line methods identify molecular aminoborane (H<sub>2</sub>N=BH<sub>2</sub>) as a species that can be released in appreciable quantities with the other major impurity, borazine. Attenuated total reflectance Fourier transform infrared spectroscopy (ATR-FTIR) was used to identify the chemical states present in the solid phase material after each stage of decomposition. The boron nitride product was examined for composition, structure, and morphology using scanning Auger microscopy (SAM), powder X-ray diffraction (XRD), and field emission scanning electron microscopy (FESEM). Thermogravimetric Analysis–Mass Spectroscopy (TGA-MS) and Differential Scanning Calorimetry (DSC) were used to identify the onset temperature of the first two mass loss events.

### Introduction

Ammonia borane (H<sub>3</sub>N–BH<sub>3</sub>) is a molecular solid currently being investigated as a chemical hydrogen storage material because of its high hydrogen content (19.6 wt %) and favorable hydrogen release characteristics. Two temperature dependent pyrolysis steps that each release about 1 mol equivalent of H<sub>2</sub> per mole of ammonia borane (AB) are generally accepted to occur at 110 and 130 °C.<sup>1–5</sup> To our knowledge, a third mass loss onset temperature has not been well-defined. Here we report a third major mass loss event beginning at 1170 °C in a nitrogen atmosphere that results in

a semicrystalline hexagonal boron nitride (hBN) after treatment at 1500 °C for 24 h in N<sub>2</sub>.

Empirical formula determinations, vibrational spectroscopy, and <sup>11</sup>B magic angle spinning–nuclear magnetic resonance (<sup>11</sup>BMAS-NMR) studies performed by other researchers have provided evidence that a complex, branched form of polyaminoborane (PAB),  $-\text{[NH}_2\text{–BH}_2\text{]}_n-$ , is formed in the solid phase during the first hydrogen release step.<sup>2,6,7</sup> In separate studies, preparations of PAB decompose over a broad range of temperatures to form structures approximating polyiminoborane, (PIB)  $-\text{[NH=BH]}_n-$ .<sup>5</sup> Small amounts of gas phase species which form in addition to hydrogen, such as borazine (N<sub>3</sub>B<sub>3</sub>H<sub>6</sub>) account for mass losses observed in TGA experiments that cannot be solely attributable to hydrogen evolution. Baitalow et al. demonstrated constant hydrogen production, and variable mass loss at different heating rates,<sup>2</sup>

\*To whom correspondence should be addressed. E-mail: steven.suib@uconn.edu.

(1) Hu, M. G.; Geanangel, R. A.; Wendlandt, W. W. *Thermochim. Acta* **1978**, *23*, 249–55.

(2) Baitalow, F.; Baumann, J.; Wolf, G.; Jaenicke-Rössler, K.; Leitner, G. *Thermochim. Acta* **2002**, *391*, 159–168.

(3) Sit, V.; Geanangel, R. A.; Wendlandt, W. W. *Thermochim. Acta* **1987**, *113*, 379–382.

(4) Wolf, G.; Baumann, J.; Baitalow, F.; Hoffmann, F. P. *Thermochim. Acta* **2000**, *343*, 19–25.

(5) Baumann, J.; Baitalow, F.; Wolf, G. *Thermochim. Acta* **2005**, *430*, 9–14.

(6) Bowden, M.; Kemmitt, T.; Shaw, W.; Hess, N.; Linehan, J.; Gutowski, M. et al. Mechanistic Studies of Hydrogen Release From Solid Amine Borane Materials. *Proceedings Materials Research Society Symposium*, San Francisco, CA, April 17–19, 2006.

(7) Stowe, A. C.; Shaw, W. J.; Linehan, J. C.; Schmid, B.; Autrey, T. *Phys. Chem. Chem. Phys.* **2007**, *9*, 1831–1836.

suggesting that reaction kinetics are an important factor in dictating the formation of impurity gases.<sup>1–5</sup>

A number of recent studies have focused on chemical analogues of ammonia borane.<sup>8–10</sup> The compounds  $\text{LiNH}_2\text{BH}_3$  and  $\text{NaNH}_2\text{BH}_3$  were reported by Xiong et al. to evolve hydrogen in a single exothermic step near 90 °C, without detectable evolution of borazine.<sup>8</sup> Wu et al. have determined the crystal structure of these metal amidoboranes.<sup>9</sup> Sneddon and Yoon have examined ammonia triborane as a potential hydrogen storage material.<sup>10</sup>

In this study, the thermal decomposition of ammonia borane was studied using a variety of methods to qualitatively identify gas and remnant solid phase species after thermal treatments up to 1500 °C. Attenuated total reflectance Fourier transform infrared spectroscopy (ATR-FTIR) is used to determine chemical structures in the residual solid phase material present after each of the three known decomposition steps. The residual boron nitride was characterized by powder X-ray Diffraction (XRD) and scanning Auger microscopy (SAM) to determine structure and composition. The boron nitride was also characterized by field emission scanning electron microscopy (FESEM) to determine morphology. Gas evolution and thermochemistry were quantified by vacuum line techniques, thermogravimetric analysis (TGA), and differential scanning calorimetry (DSC). The temperature dependence of hydrogen and impurity gas evolution was studied using mass spectroscopy.

A specific long-term goal of this research is to produce a fuel element that contains solid reactants for the generation of  $\text{H}_2$  fuel. Under development is the use of ammonia borane as a hydrogen source. The ammonia borane is to be held in a housing where electrical leads are used to ignite a small pyrotechnic charge which initiates a self-propagating thermal decomposition reaction throughout the fuel element, releasing the hydrogen.<sup>11</sup>

## Experimental Methods

**(A). Materials.** High purity Ammonia borane powder was obtained from Ensign Bickford Aerospace and Defense. Samples were stored in desiccators or an argon drybox. Ultrahigh purity (UHP) grade Helium, Argon, and  $\text{N}_2$  were obtained from Airgas. Anhydrous ammonia (99.99%) was also obtained from Airgas. Borazine was obtained from Borosciences Canada. Hexagonal boron nitride (hBN) was obtained from Alfa Aesar (99.5%, lot F09P16).

**(B). Thermogravimetric Analysis (TGA).** Because of the tendency of AB to significantly expand in volume during pyrolysis, sample mass was limited to less than 2 mg for all TGA experiments. Thermogravimetric analyses were conducted on three instruments. The first instrument, a TA Instruments TGA Q500, was enclosed within an argon filled glovebox to eliminate the presence of trace atmospheric gases in the thermobalance during analysis. The second instrument, a TA Instruments TGA 2950, was housed in the open atmosphere on a benchtop. These two instruments have nearly identical furnace and balance configurations. Samples were loaded into weight tared platinum

pan, and the temperature was ramped at 5 °C/min from 23 to 450 °C under flowing Argon.

The third instrument, used for high temperature studies, was a TA Instruments TGA Q600. The sample was loaded into a weight tared alumina pan, and ramped at 25 °C/min to 1500 °C under flowing nitrogen. A 25 min isothermal period at 98 °C was included to prevent excessively rapid mass loss at the melting point because of the otherwise high heating rate. Operational parameters of the Q600 instrument required a heating rate of 5 °C/min above 1485 °C.

**(C). Thermogravimetric Analysis-Mass Spectroscopy (TGA-MS) and Temperature Programmed Desorption-Mass Spectroscopy (TPD-MS).** TGA-MS experiments were carried out using the TA Instruments TGA Q500, enclosed within an argon filled glovebox. Mass spectroscopic analysis of gases exiting the thermobalance was carried out with an MKS model quadrupole residual gas analyzer (RGA) using a 40 eV electron impact ionization source. The quadrupole was used to scan all  $m/z$  ratios from  $m/z = 1$  to  $m/z = 90$  approximately every 30 s.

TPD-MS experiments were conducted on a home-built apparatus which could accommodate a larger sample size than the TGA-MS instrument, thus allowing detection of impurity level gases. An MKS E-Vision<sup>+</sup> model RGA was used with a 40 eV electron impact ionization source. Samples (50 mg) were loaded into a 9 mm outer diameter (O.D.) and 7 mm inner diameter (I.D.) quartz tube reactor. Helium carrier gas (50 sccm) was delivered through PFA tubing connected to the quartz tube via Swagelok and Ultra-Torr brand compression fittings. The vacuum system of the RGA was continuously sampled from species present at a “T” in the exit gas line from the quartz tube. Temperature was controlled by a resistively heated tube furnace and a type K thermocouple in thermal contact with the external surface of the quartz tube at the location of the sample.

The sample was heated at 25 °C/min, held at 114 °C for 120 s, and then heated again at 25 °C/min to 135 °C where the temperature was held for another 120 s. At least 3 scans from  $m/z = 1$  to  $m/z = 90$  were recorded during both isothermal periods, averaged, and plotted after a baseline subtraction.

**(D). Borazine Mass Spectrum.** Borazine vapor was introduced into a lecture bottle. The lecture bottle was connected to a “T” in a helium carrier gas line. The borazine vapor was entrained by the flowing helium carrier gas, and this mixture was carried to the inlet of the MKS E-vision<sup>+</sup> residual gas analyzer.

**(E). Differential Scanning Calorimetry.** Differential scanning calorimetry (DSC) experiments were carried out on a TA Q100 system. Ammonia borane was weighed in an aluminum pan which was then crimped closed. A pinhole allowed the escape of evolved gases. Ramp rates of 5 °C/min to 400 °C were used with an  $\text{N}_2$  purge gas after an initial 30 min isothermal period at 40 °C to remove atmospheric gases and adsorbed moisture.

**(F). Preparation of Solid Phase Ammonia Borane Pyrolysis Products.** Under controlled atmospheres, AB was thermally treated at three different temperatures, 120, 210, and 1500 °C, referred to as AB-120 °C, AB-210 °C, and AB-1500 °C, respectively. AB-120 °C and AB-210 °C were generated by immersing Pyrex vessels containing the compound into heated oil baths for 5 min under UHP helium carrier gas. The materials generated were stored in helium atmosphere until immediately prior to analysis by ATR-FTIR. A third sample was prepared by treatment of AB at 1500 °C for 24 h in a high temperature tube furnace in an alumina sample holder under UHP nitrogen carrier gas.

**(G). ATR-FTIR Spectroscopy.** A Spectra Tech IR Plan model microattenuated total reflectance (ATR) Fourier transform infrared (FTIR) spectrometer with a Nicolet Magna 560 light source and detector was used to obtain IR spectra. The spectra of ammonia borane and the three solid phase pyrolysis products prepared as described above were obtained. In addition,

(8) Xiong, Z.; Yong, C. K.; Wu, G.; Chen, P.; Shaw, W.; Karkamkar, A.; et al. *Nat. Mater.* **2008**, *7*, 138–141.

(9) Wu, H.; Zhou, W.; Yildirim, T. *J. Am. Chem. Soc.* **2008**, *130*, 14843–14839.

(10) Yoon, C. W.; Sneddon, L. G. *J. Am. Chem. Soc.* **2006**, *128*, 13992–13993.

(11) Boucher, C.; Mallery, C.; Mecca, L.; Korcsmaros, R. Thermite-activated thermal decomposition of ammonia borane-containing module for hydrogen generation, PCT Int. Appl., 23 pp, WO 2007098271, 2007.

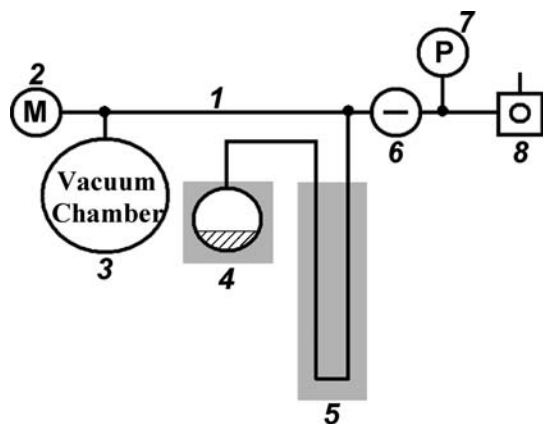


**Figure 1.** Vacuum system for quantification of  $\text{H}_2$  evolution from ammonia borane: (1) manifold constructed of 9 mm (outside diameter) pyrex tubing; (2) mercury monometer; (3) 2000 mL Pyrex vacuum chamber; (4) sample holder heated by immersion into a 240 °C silicone oil bath; (5) liquid nitrogen trap to condense non-hydrogen gas phase species; (6) vacuum stopcock; (7) Pirani vacuum gauge; (8) mechanical vacuum pump.

the spectrum of the hexagonal phase boron nitride from Alfa Aesar was obtained.

**(H). Powder X-ray Diffraction.** Powder XRD patterns were obtained using a Scintag model XDS 1000. The scan rate was 0.5 deg  $2\theta$ /min. An aluminum sample holder was used.

**(I). Auger Spectroscopy.** Auger spectra were acquired using a Physical Electronics PHI 610 scanning Auger microprobe. The powdered AB-1500 °C and commercial hBN samples were embedded into Indium foil. The samples also were sputtered with  $\text{Ar}^+$  ions. The following conditions were used: Tilt = 45° WRT incident electron beam, energy analyzer resolution = 0.6%.  $P_{\text{Base}} \leq 8.2 \times 10^{-9}$  mm Hg,  $E_p = 3.0$  keV,  $I_{e^-} = 10$  nA,  $E_{\text{Ar}^+} = 4.0$  keV,  $I_{\text{Ar}^+} = 1.0$   $\mu\text{A}$ ,  $A_{\text{Raster}} \approx 7.5$  mm<sup>2</sup>,  $\text{Time}_{\text{Sputter}} = 20.0$  min<sup>6</sup>. The symbol  $P_{\text{Base}}$  is the system pressure during data acquisition (excluding  $P_{\text{Ar}}$  while sputtering with  $\text{Ar}^+$ ),  $E_p$  is the energy of the incident electron beam,  $I_{e^-}$  is the electron beam current measured at sample with +90 V bias applied,  $E_{\text{Ar}^+}$  is the energy of the incident  $\text{Ar}^+$  beam,  $I_{\text{Ar}^+}$  is the  $\text{Ar}^+$  ion beam current measured at the sample with +90 V bias applied,  $A_{\text{Raster}}$  is the area rastered by the ion beam, and  $\text{Time}_{\text{Sputter}}$  is the Total  $\text{Ar}^+$  sputtering time. A lower electron beam energy was not used since the calculated concentrations tend to be less accurate. Because sample charging was so severe, it was necessary to use the smallest electron beam current that normally is feasible for data acquisition. Detail spectra as well as survey spectra were acquired. Peak intensities in detailed spectra are defined as the difference between the maximum and minimum values of the derivative plot.

**(J). Field Emission Scanning Electron Microscopy.** FESEM images of AB-1500 °C and the crystalline hBN from Alfa Aesar were obtained using a Zeiss DSM 982 Gemini with a Schottky emitter and a secondary electron detector. The electron beam energy was 2 kV. The powders were mounted onto the sample stub using double sided carbon tape. Excess powder was gently blown off the tape with compressed air.

**(J). Vacuum Experiments.** Ammonia borane was decomposed under vacuum conditions in a closed, constant volume system for quantitative measurements of  $\text{H}_2$  evolution. [Figure 1] Attachments of the different components were made with standard ground glass joints. The volume of the entire system was determined by using ideal gas law calculations. The base pressure was 1 mtorr. The system was isolated by closing the vacuum stopcock. The reaction flask containing ammonia borane was then heated to 240 °C by immersion in a silicone oil bath. Gases generated in the reaction flask passed through a

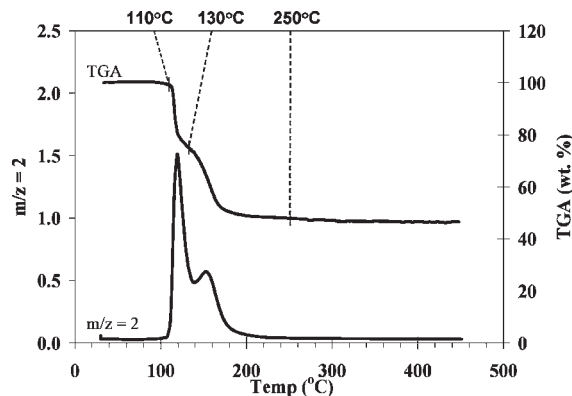


**Figure 2.** TGA-MS.

liquid nitrogen trap before entering the manifold. Borazine and any other condensable gases remained in the trap. The number of mols of  $\text{H}_2$  evolved was calculated from measurements of the final pressure with a small correction factor applied because of the cooling effect of the liquid  $\text{N}_2$ .

## Results

### Thermogravimetric Analysis and Mass Spectroscopy.

**TGA-MS.** The mass loss profiles of ammonia borane and the  $m/z = 2$  signal recorded by the mass spectrometer during the TGA-MS experiment to 400 °C are overlaid in Figure 2. These data were collected with the TGA system in a glovebox under argon gas. At a heating rate of 5 °C/min in Ar atmosphere there is an onset temperature at 108 °C and a second onset is initiated at about 130 °C. Around 210 °C, mass loss stabilizes at 50 wt %. Mass loss and  $\text{H}_2$  evolution were closely associated. Ammonia borane contains 19.3% hydrogen by mass; however, no other gas phase species were detected. Presumably, the small, 1.5 mg sample size did not evolve nitrogen and boron containing molecules into the carrier gas at detectable levels. Nitrogen or boron species have a greater per molecule effect on mass loss than  $\text{H}_2$  and are also more likely to form condensed phases in the tubing prior to reaching the mass spectrometer sampling inlet. Larger sample sizes were used for TPD-MS experiments, and nitrogen and boron containing molecules were evolved and detected.

**TPD-MS.** Baseline subtracted mass spectra of pyrolysis gases obtained during isothermal periods at 114 and 135 °C clearly indicate  $\text{H}_2$  is the most abundant gas phase pyrolysis species but that other species are also present in both cases. After rapid heating to 114 °C [Figure 3A] the presence of species at 27, 28, and 29 amu is identified. After rapidly heating this sample again to 135 °C, [Figure 3B] mass fragments consistent with those obtained from pure borazine [Figure 3C] and increased levels of the 27, 28, and 29 amu species were detected. A small peak at 87 amu was also detected. The 2 amu signals are at least an order of magnitude larger than signals produced by any other mass. It was typical for a white coating to form on the interior walls of the quartz tubing at the exit of the furnace. This coating evolved additional hydrogen, borazine, and molecular aminoborane when gently heated with a Bunsen burner flame.

**Borazine Mass Spectrum.** The isotopic distribution of boron causes molecular ion and deprotonation peaks to overlap. The most intense peak of the pure borazine mass

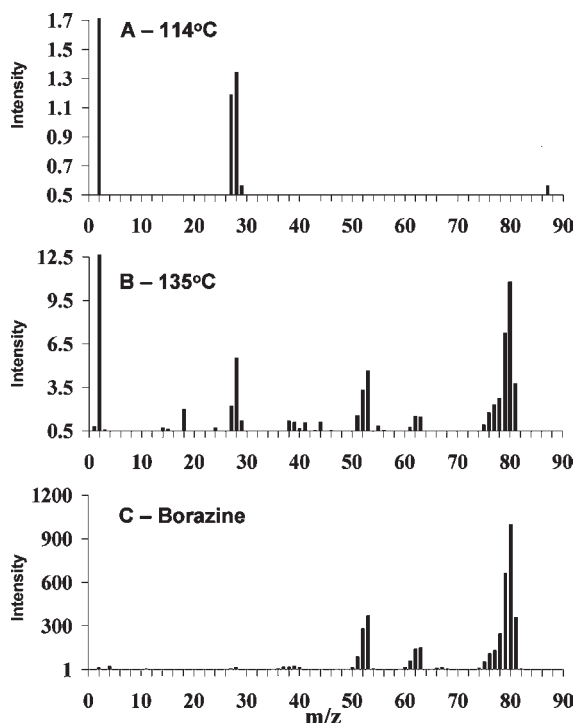


**Figure 3.** Mass Spectrum: (A) pyrolysis gases generated at 114 °C scaled to impurity levels; (B) pyrolysis gases generated at 135 °C scaled to impurity levels; (C) pure borazine. The  $m/z = 2$  signal intensities in A and B are each about 2 orders of magnitude above their respective  $y$ -axis scales.

spectrum at 80 amu [Figure 3C] corresponds to the mass of the 80 amu molecular ion, and deprotonation of the most abundant 81 amu molecular ion. The 81 amu borazine species is statistically the most abundant molecular weight for borazine. Other fragment clusters were observed around 67 amu, 63 amu, 53 and 28 amu. There was no contribution at 29 amu, and only small contributions at 26, 27, and 28 amu.

**TGA: The Glove Box Effect.** When the thermobalance was not housed within a glove we typically obtained mass loss curves that deviated at the second mass loss step. [Figure 4] A thermobalance housed within an argon filled glovebox was able to eliminate these deviations and mass increases.

**TGA to 1500 °C.** TGA data in Figure 5 for ammonia borane heated to 1500 °C in nitrogen atmosphere at a 25 °C/min ramp rate record the mass loss associated with the first two well-known decomposition steps. A 25 min isotherm was included at 98 °C, and mass loss was observed during this period. A third major mass loss event was initiated at 1170 °C, and decomposition was still occurring at 1500 °C, the maximum operating temperature of the instrument.

**Differential Scanning Calorimetry.** DSC data for pure ammonia borane in nitrogen are shown in Figure 6. The heat flow per gram of starting mass of sample is  $-0.68$  W/g at 110 °C;  $-9.61$  W/g at 116 °C;  $-1.45$  W/g at 170 °C; and  $-0.56$  W/g at 397 °C. An endothermic transition initiates at 110 °C followed by an exothermic transition at 120 °C followed by another endothermic transition at 135 °C.

**Vacuum Line Hydrogen Quantifications.** Rapidly heating ammonia borane to 240 °C released an amount of

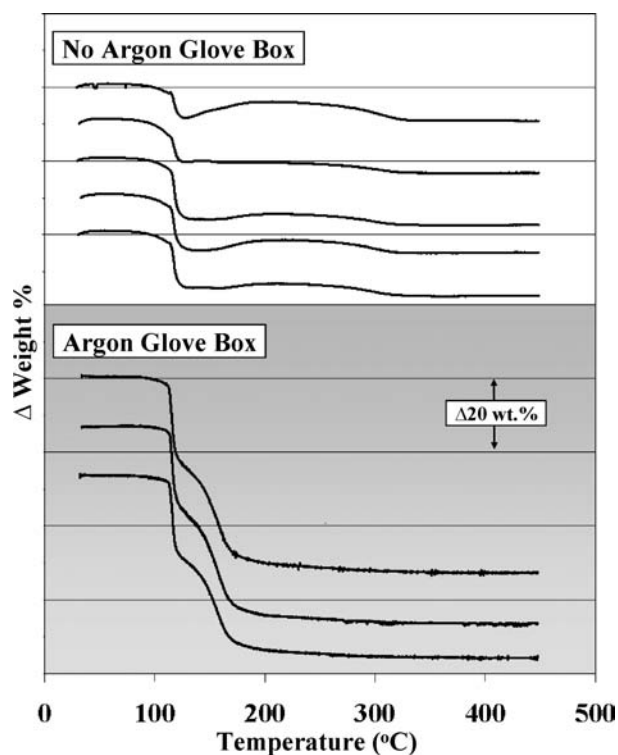


**Figure 4.** TGA curves: The glovebox effect. Three TGA curves obtained from an instrument housed in an argon filled glovebox (shaded area) are stacked against five TGA curves obtained from an instrument housed in the open atmosphere (unshaded area). Horizontal line spacing corresponds to a 20 wt % change. The heating rate was 5 °C/min in Ar carrier gas to 450 °C.

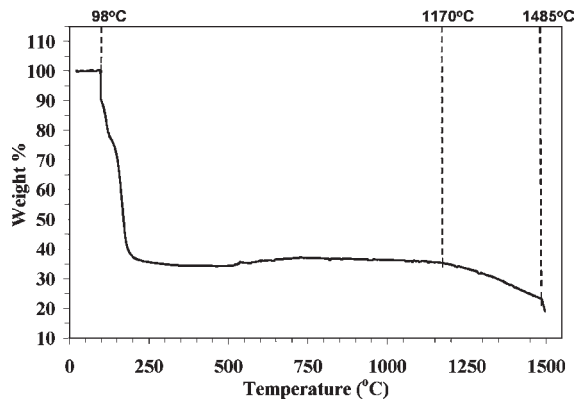


**Figure 5.** TGA to 1500 °C in  $N_2$ . Heating rate was 25 °C/min. Above 1485 °C the heating rate was 5 °C/min. A 25 min isotherm was included at 98 °C.

$H_{2(g)}$  equal to 10.5% of the original sample mass, or 1.61 mol equivalents. Roughly 95% of the hydrogen evolved in less than one minute. After 5 min, no more hydrogen evolution could be observed. When the sample holder was immersed in silicone oil, the ammonia borane melted within several seconds. Vigorous bubbling occurred immediately within the melt. Within seconds, the melt solidified to a white material. In similarity to TPD-MS experiments, a white film coated the inside walls of the Pyrex tubing between the sample holder and the liquid nitrogen trap, (between points 4 and 5 in Figure 1). This material was found to produce additional hydrogen when gently heated with a Bunsen burner flame.

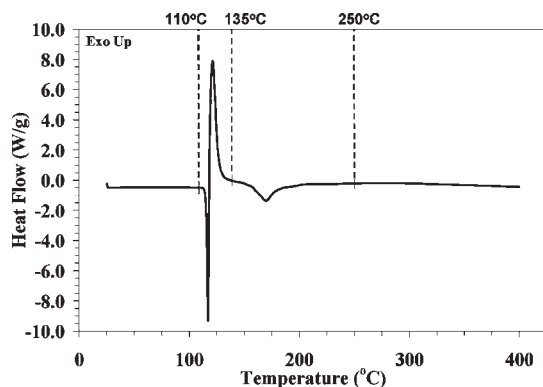


Figure 6. DSC curve: Ammonia Borane, 5 °C/min in N<sub>2</sub> to 400 °C.

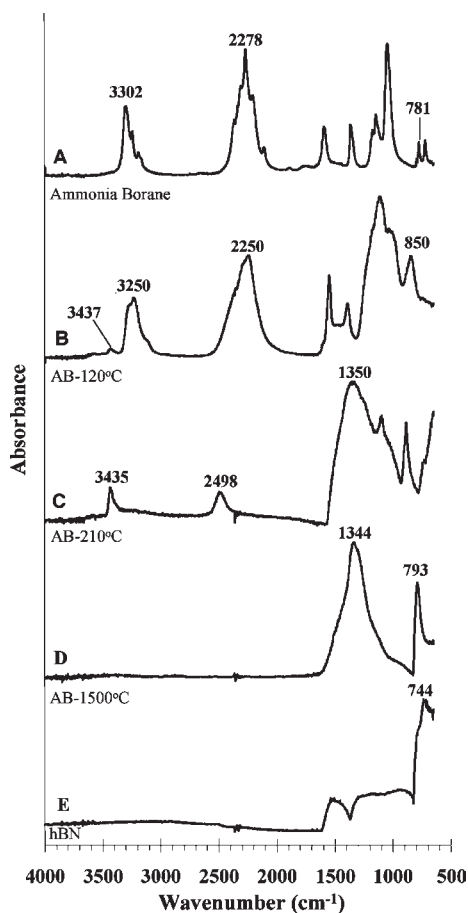


Figure 7. ATR-FTIR spectra of solid phase decomposition products and hexagonal boron nitride: (A) room temperature ammonia borane; (B) ammonia borane treated at 120 °C; (C) ammonia borane treated at 210 °C; (D) ammonia borane treated at 1500 °C; (E) hBN.

If stored in an argon drybox at atmospheric pressure, the white coating persisted for several months. If exposed to room air, the white coating visibly decomposed within minutes. A protected environment would be required to obtain spectral data for this material.

**ATR-FTIR.** Band positions in the ATR-FTIR spectra [Figure 7] of untreated, room temperature ammonia borane match well with those from previously published vibrational spectroscopy studies of the compound. The absorbance peaks at 3302 cm<sup>-1</sup> and 2278 cm<sup>-1</sup> in ammonia borane are shifted to a slightly lower wavenumber in

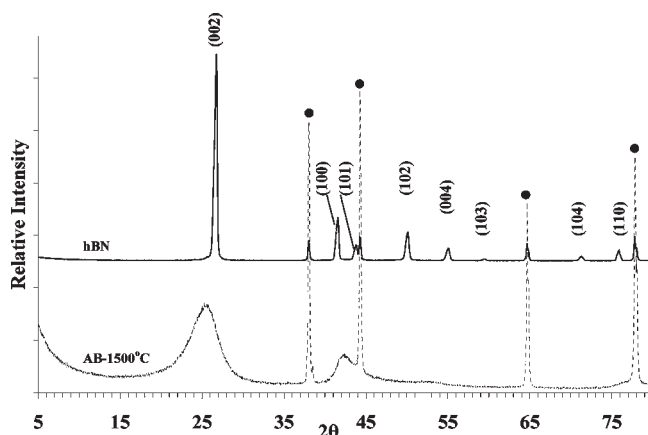


Figure 8. Powder X-ray diffraction of hexagonal phase boron nitride and ammonia borane treated at 1500 °C (AB-1500 °C). Sample holder peak positions, indicated by bullets (●), and by dashed lines.

AB-120 °C. A small peak at 3437 cm<sup>-1</sup> also appears in AB-120 °C. These bands shift position again to 3435 cm<sup>-1</sup> and 2498 cm<sup>-1</sup> in AB-210 °C and also exhibit a decrease in their relative intensity. In AB-1500 °C, and the commercial hBN sample, no bands are present above 1700 cm<sup>-1</sup>. There are a number of overlapping, complex bands present in each spectrum below 1700 cm<sup>-1</sup>.

**Powder X-ray Diffraction.** The Powder XRD pattern [Figure 8] obtained from the commercial hBN sample was closely indexed to the JCPDS card file 34-0421 for space group *P63/mmc* hBN. All reflections arising from the AB-1500 °C material are weak and broad, but occur in coincidence with the locations and relative intensities of the sharp peaks in the commercial hBN sample. Reflections arising from the aluminum sample holder are identified in both patterns.

**Scanning Auger Microscopy.** Two samples, AB-1500 °C and a commercial hBN, were subjected to elemental analysis by SAM to compare atomic composition. Representative survey spectra of the two samples are displayed in Figure 9. Attempts to obtain SAM spectra after Ar<sup>+</sup> sputtering were unsuccessful because of sample charging. After Ar<sup>+</sup> sputtering, charge accumulated on the sample with the application of the e-beam preventing spectra from being acquired. The adventitious carbon may have provided a conductive pathway for charge dissipation. Spectra without a carbon signal were not possible to obtain. Oxygen, nitrogen, boron, and carbon were found in each sample by the presence of KLL transitions from each atom. Relative peak intensities obtained from detailed spectra at multiple spots are listed in Table 1.

**Scanning Electron Microscopy.** The crystalline hBN sample [Figure 10a] is composed of micrometer sized platelets typical of highly crystalline hBN. The topology of AB-1500 °C [Figures 10b and 10c] is non-uniform and discontinuous at a 100 nm scale. The AB-1500 °C particles have not adopted a uniform, regular shape. The AB-1500 °C particle size ranges from 1 μm to over 100 μm.

**Decomposition Under Anhydrous Ammonia.** A second sample of ammonia borane was ramped to 1500 °C under a pure anhydrous ammonia carrier gas, and held at that temperature for 24 h in an alumina tube and alumina sample boat. There was no significant difference in the

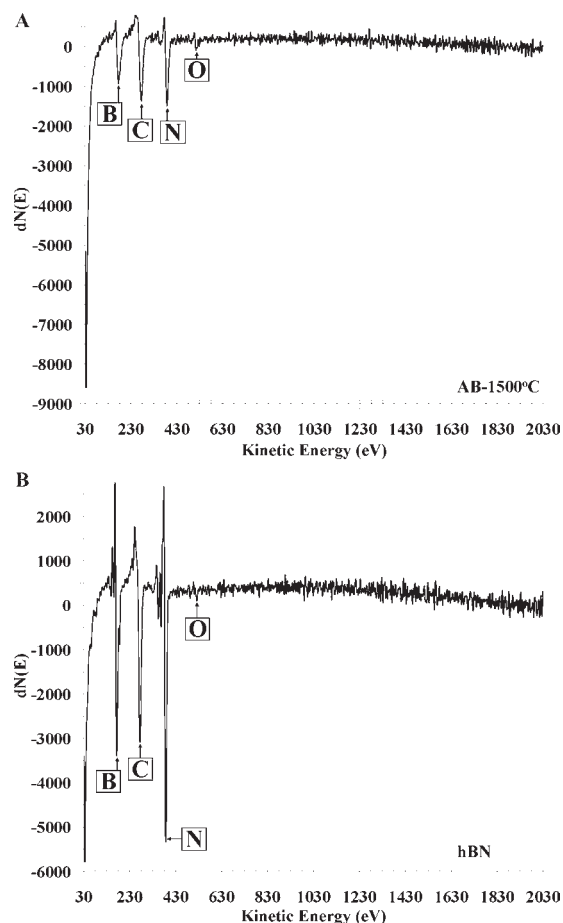


**Figure 9.** B, C, N, and O KLL Auger Electrons in SAM survey spectra: (A) ammonia borane treated at 1500 °C; (B) the commercially available hexagonal boron nitride powder.

**Table 1.** Scanning Auger Microscopy: Normalized B, N, C, and O, KLL Peak Intensities

	sample					
	AB-1500 °C			P63/mmc hBN		
	spot					
	1	2	3	1	2	3
B	25	2433	18	27	27	26
N	29	30	26	32	32	33
C	41	40	51	41	39	40
O	6	6	5	1	2	1

N:B 1.19 1.23 1.45 1.19 1.21 1.25

The composition of ammonia borane powder treated at 1500 °C is nearly identical to the hBN reference powder. Three spots from each sample were examined. Spectra could not be obtained after the sample was Ar<sup>+</sup> sputtered to remove adventitious carbon. Carbon impurity is the likely explanation for variation in spot 3 of AB-1500 °C. The sums of peak intensities from each spot are normalized to a value of 100. N:B is the nitrogen to boron peak intensity ratio.

XRD pattern or the ATR-FTIR spectrum of the resultant material in comparison to AB-1500 °C, prepared under identical circumstances with a nitrogen carrier gas.

## Discussion

**Thermogravimetric and Evolved Gas Analysis. High Temperature TGA: Toward Boron Nitride.** According to

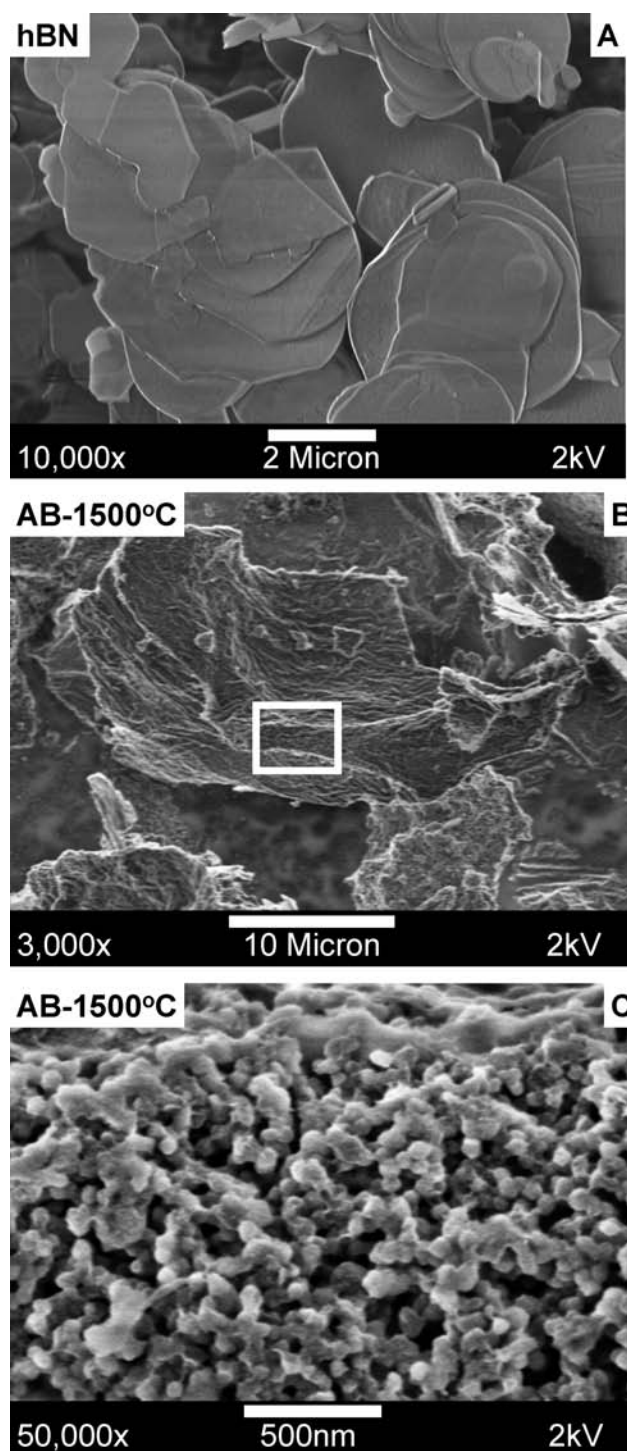


**Figure 10.** Secondary electron FESEM images: (A) commercially available hexagonal boron nitride; (B) AB-1500 °C; (C) AB-1500 °C, the enclosed area in panel B.

TGA data of Figure 5, a major mass loss event was initiated at 1170 °C, and was still occurring at 1500 °C, the maximum operating temperature of the instrument. This is in agreement with a report that a polyaminoborane pre-ceramic polymer undergoes hydrogen loss at an unknown point between 1000 and 1400 °C.<sup>12</sup> The kinetics of the third mass loss step are significantly slower than either of

(12) Kim, D.; Moon, K.; Kho, J.; Economy, J.; Gervais, C.; Babonneau, F. *Polym. Adv. Technol.* **1999**, *10*, 702–712.

the first two mass loss steps. The high onset temperature and slow rate of the third mass loss effectively limits the amount of hydrogen available from ammonia borane by thermal pyrolysis. The 2%–3% mass gain initiating at 500 °C is probably due to slight mass measurement error at elevated temperatures.

**TGA-MS.** A mass of 2 mg was used in the TGA-MS experiments. The TGA-MS data of Figure 2 demonstrate the first two well-known onset points at 108 and 125 °C occur in coincidence with an increase in hydrogen evolution. The two mass loss events are not completely separated at the 5 °C/min heating rate used in this experiment although the occurrence of a second onset strongly implies the existence of two distinct temperature dependent chemical events. On the basis of peak areas, roughly equal amounts of hydrogen were evolved in each of the two steps.

A 50% total weight loss can not be accounted for entirely by hydrogen evolution alone; however, the mass spectrometer did not detect any other species. This is presumably because impurities occurred below detection limits. TPD-MS experiments using larger sample sizes detected the evolution of multiple nitrogen and boron containing species at low levels.

**TPD-MS and the Pure Borazine Spectrum.** Comparison of the mass spectrum of non-hydrogen pyrolysis gases, generated during the TPD-MS experiment to the mass spectrum of pure borazine, clearly identify a temperature dependent evolution of impurity gases and the evolution of molecular aminoborane, in addition to borazine. [Figure 3] Pyrolysis gases generated at 114 °C contain molecular aminoborane at low levels, as evidenced by the presence of a peak at 29 amu, because of molecular aminoborane with a <sup>11</sup>B isotope. The relative intensities of the peaks at 26–29 amu match a previously obtained electron impact ionization mass spectrum of aminoborane.<sup>13</sup> The peak at 87 amu could be an aminoborane trimer. During TPD-MS experiments a white particulate film consistently coated the interior walls of the exit tube. On gentle heating with a Bunsen burner, this film was found to evolve hydrogen, borazine, and molecular aminoborane, but was *not* completely volatilized off the tubing wall.  $\pi$  bonded nitrogen and boron atoms do not readily evolve hydrogen. In light of this information, the most plausible sources of this white film are physically and chemically condensed low molecular weight volatiles with a stoichiometry of NBH<sub>x</sub> where  $x \geq 2$ . This includes species such as ammonia borane, molecular aminoborane, and low molecular weight polymers of PAB. At the low temperatures outside the furnace, gas phase molecular aminoborane could polymerize to a solid phase PAB type structure. Similar results obtained with the vacuum line experiments are discussed elsewhere in this article.

**Glove-Box TGA and DSC.** The presence of trace atmospheric gases influenced the TGA curves in relation to the reproducible results obtained from UHP argon conditions. Adsorbed species like H<sub>2</sub>O and O<sub>2</sub> could suppress desorption of H<sub>2</sub> by interacting with surface sites on the decomposing ammonia borane.

The DSC data [Figure 6] were not collected with the instrument housed in a glovebox but measures were taken

**Table 2.** Dependence of Stretching Frequencies on Bond Order for BNH Compounds<sup>a</sup>

compound	ref	BO	NH <sup>st</sup> (cm <sup>-1</sup> )	BH <sup>st</sup> (cm <sup>-1</sup> )	BN <sup>st</sup> (cm <sup>-1</sup> )
H <sub>3</sub> B-NH <sub>3</sub>	<i>b,e,f</i>	1	3167–3316	2279–2375	784–800
H <sub>3</sub> B-NH <sub>2</sub> -CH <sub>3</sub>	<i>c</i>	1	3175–3374	2367–2415	667–726
H <sub>3</sub> B-NH(CH <sub>3</sub> ) <sub>2</sub>	<i>c</i>	1	3219–3236	2260–2384	659–708
H <sub>3</sub> B-N(CH <sub>3</sub> ) <sub>3</sub>	<i>c</i>	1	none	2270–2393	648–667
H <sub>2</sub> B=NH <sub>2</sub>	<i>d</i>	2	3451–3533	2495–2564	1337
H <sub>2</sub> B=NH-CH <sub>3</sub>	<i>c</i>	2	3447	2471–2561	1314–1322
H <sub>2</sub> B=N(CH <sub>3</sub> ) <sub>2</sub>	<i>c</i>	2	none	2369–2575	1148–1229
HB=NH	<i>g,h</i>	3	3700–3712	2775–2820	1782–1822

<sup>a</sup> As bond order (BO) between the boron nitrogen bond increases, fundamental stretching mode frequencies increase. The wavenumbers listed cover the range of values assigned to stretching modes in the indicated references. <sup>b</sup> Ref 14. <sup>c</sup> Ref 15. <sup>d</sup> Ref 16. <sup>e</sup> Ref 17. <sup>f</sup> Ref 18. <sup>g</sup> Ref 19. <sup>h</sup> Ref 20.

to reduce the amount of adsorbed H<sub>2</sub>O within the DSC cell itself. The first large endothermic transition is consistent with the melting of ammonia borane. The rapid transition to an exothermic process corresponds with the rapid desorption of H<sub>2</sub> that occurs immediately on melting. The DSC data indicate an endothermic step corresponding with the second mass loss event initiating at about 135 °C. This event has been reported as an exothermic transition in other DSC studies<sup>2</sup> with an identical heating rate and carrier gas. We have repeated our experiments several times and obtained highly consistent results. Minute differences in conditions clearly have an effect on the chemical pathways and heat effects which occur during pyrolysis. This result highlights some areas of urgently needed research if ammonia borane is to be commercialized as a fuel cell hydrogen source. Our future investigations are designed to identify and quantify the influence of variables such as trace levels of atmospheric gases, purity, preparation method, grain size, agglomeration, bulk configuration, heat transfer kinetics, presence of additives, container geometry, and gas flow dynamics.

**Solid Phase Characterization. ATR-FTIR.** Changes in the fundamental N–H, B–H, and B–N stretching frequencies are particularly diagnostic of chemical state as decomposition proceeds because these frequencies tend to increase with the  $\pi$  bond character between nitrogen and boron atoms.<sup>14–20</sup> Table 2 lists selected assignments from infrared spectra of several molecular compounds with different nitrogen-boron bond orders.

The bond orders between nitrogen and boron atoms present in ammonia borane, AB-120 °C, AB-220 °C, and AB-1500 °C can be identified by the position of the NH, BH, and BN stretching frequencies in each of the materials. A determination of chemical structure of each

(14) Hess, N. J.; Bowden, M. E.; Parvanov, V. M.; Mundy, C.; Kathmann, S. M.; Schenter, G. K.; et al. *J. Chem. Phys.* **2008**, *128*, 034508/1–034508/1.

(15) Carpenter, J. D.; Ault, B. S. *J. Phys. Chem.* **1991**, *95*, 3507–3511.

(16) Gerry, M. C. L.; Lewis-Bevan, W.; Merer, A. J.; Westwood, N. P. C. *J. Mol. Spectrosc.* **1985**, *110*, 153–63.

(17) Smith, J.; Seshadri, K. S.; White, D. *J. Mol. Spectrosc.* **1973**, *45*, 327–337.

(18) (a) Klooster, W. T.; Koetzle, T. F.; Siegbahn, E. M.; Richardson, T. B.; Crabtree, R. H. *J. Am. Chem. Soc.* **1999**, *121*, 6337. (b) Bowden, M. E.; Gainsford, G. J.; Robinson, W. T. *Aust. J. Chem.* **2007**, *60*, 149–153.

(19) Thompson, C. A.; Andrews, L.; Martin, J. M. L.; El-Yazal, J. *J. Phys. Chem.* **1995**, *99*, 13839–13849.

(20) Lory, E.; Porter, R. *J. Am. Chem. Soc.* **1973**, *95*, 1766–1770.

(13) Kwon, C. T.; McGee, A. H. *Inorg. Chem.* **1970**, *9*, 2458–2461.

**Table 3.** Bond Stretch and Bond Order (BO) Assignments

sample	BO	NH <sup>st</sup> (cm <sup>-1</sup> )	BH <sup>st</sup> (cm <sup>-1</sup> )	BN <sup>st</sup> (cm <sup>-1</sup> )
AB-RT	1	3302	2278	781
AB-120 °C	1	3250	2250	850
	2	3437		
AB-210 °C	2	3435	2498	1344
AB-1500 °C	1.33	none	none	1338
hBN	1.33	none	none	~1300

The bond order (BO) present between nitrogen and boron atoms can be ascertained by IR absorbance peak positions. The formation of nitrogen–boron double bonds (BO = 2) begins to occur at about 120 °C. Boron to nitrogen bonds of BO = 1 and BO = 2 are both present in AB-120 °C. The NH<sup>st</sup> and BH<sup>st</sup> peak positions in this table include contributions from multiple fundamental stretching modes, and are diagnostic of bond order. BN<sup>st</sup> peaks overlap with other bending modes.

material follows from knowledge of hydrogen loss and the bond orders present. Table 3 lists selected assignments from the infrared spectra we have obtained. A more detailed discussion of structural determinations obtained from the spectra follows below.

**ATR-FTIR: Ammonia Borane.** An early vibrational spectroscopy study of argon matrix isolated ammonia borane by Smith et al.<sup>17</sup> was thorough, but has been somewhat updated and revised. Infrared absorbance data observed in AB-RT of Figure 7a can be assigned on the basis of currently accepted experimental and calculated vibrational spectra of ammonia borane.<sup>14,18,21</sup> The position of stretching frequencies in ammonia borane is consistent with boron and nitrogen atoms in tetrahedral environments bonded by a coordinate covalent single bond [Table 3]. The peaks near 3302 cm<sup>-1</sup> are assigned to NH stretching modes and those near 2278 cm<sup>-1</sup> are assigned to BH stretching modes. The B–N stretching mode is observed at 781 cm<sup>-1</sup>. The peaks at 1601 cm<sup>-1</sup> and 1371 cm<sup>-1</sup> are due to NH<sub>3</sub> deformations, and a pair of partially resolved peaks at 1155 and 1180 cm<sup>-1</sup> is assigned to BH<sub>3</sub> deformations. The peaks at 1055 cm<sup>-1</sup> and 727 cm<sup>-1</sup> have been assigned to NBH rocking modes.

**ATR-FTIR: AB-120 °C.** After the evolution of significant quantities of hydrogen by treatment at 120 °C, the stretching frequency positions in AB-120 °C [Table 3] indicate the material is composed mostly of tetrahedral, singly bonded nitrogen, and boron atoms. This is strongly suggestive of a PAB, -(NH<sub>2</sub>-BH<sub>2</sub>)<sub>n</sub>-, based structure with an NBH<sub>x</sub> stoichiometry, where  $x \leq 4$ . A highly branched or cyclized PAB polymer, where  $x$  is less than 4, may have a very similar IR spectrum without significant shifts in stretching frequencies from the purely linear case.

A small peak at 3437 cm<sup>-1</sup> appears in the AB-120 °C spectrum and is assigned to NH stretching modes involving nitrogen atoms  $\pi$  bonded to adjacent boron atoms in short segments of a PIB, -(HN=BN)<sub>n</sub>-, type chemical structure, or to terminal =NH<sub>2</sub> groups of a PAB polymer. The NH and BH stretching mode peak positions decreased slightly from the ammonia borane case. This reflects the loss of the high symmetry stretching modes in ammonia borane that cannot exist in PAB.

Detailed ab initio investigations by Jacquemin et al.<sup>22</sup> on the vibrational structure of PAB predict the umbrella mode of terminal NH<sub>3</sub> groups to have a frequency of 1380 cm<sup>-1</sup> and the BN stretching mode to have a frequency 900 cm<sup>-1</sup>.

On this basis the strong peak at 850 cm<sup>-1</sup> in AB-120 °C was assigned to the BN stretching vibration involving tetrahedral nitrogen and boron atoms, and the peak at 1394 cm<sup>-1</sup> is assigned to the NH<sub>3</sub> umbrella vibration. Since the variation in dipole moment is very large with the NH<sub>3</sub> umbrella mode, NH<sub>3</sub> should be detectable in very small quantities. The peak centered at 1119 cm<sup>-1</sup> with a shoulder at 1035 cm<sup>-1</sup> is probably due to multiple unresolved bending modes possibly including a BH<sub>2</sub> deformation and a BH<sub>3</sub> umbrella.<sup>22,23</sup>

Absorptions near 1550–1600 cm<sup>-1</sup> reported elsewhere for cyloaminoborane species and the H<sub>3</sub>B-NH<sub>2</sub>-CH<sub>3</sub> adduct are assigned to NH<sub>2</sub> deformations in each case.<sup>22,23</sup> The peak at 1556 cm<sup>-1</sup> in the AB-120 °C spectrum is thus explained by an NH<sub>2</sub> deformation.

**ATR-FTIR: AB-210 °C.** The absorption bands at 3435 cm<sup>-1</sup> and 2498 cm<sup>-1</sup> and 1350 cm<sup>-1</sup> in Figure 7c are each respectively consistent with NH, BH, and BN stretching modes involving  $\pi$  bonded nitrogen and boron atoms. This strongly implies a chemical structure approximating PIB, and an NBH<sub>x</sub> stoichiometry where  $x < 2$ . A branched or cyclized PIB polymer where  $x$  is less than 2 would have a very similar IR spectrum without significant shifts in the stretching frequencies in comparison to the pure linear case. The terminal functional groups =NH and =BH are not present in the PIB structure because absorption bands near 3700 cm<sup>-1</sup> and 2800 cm<sup>-1</sup> are absent.

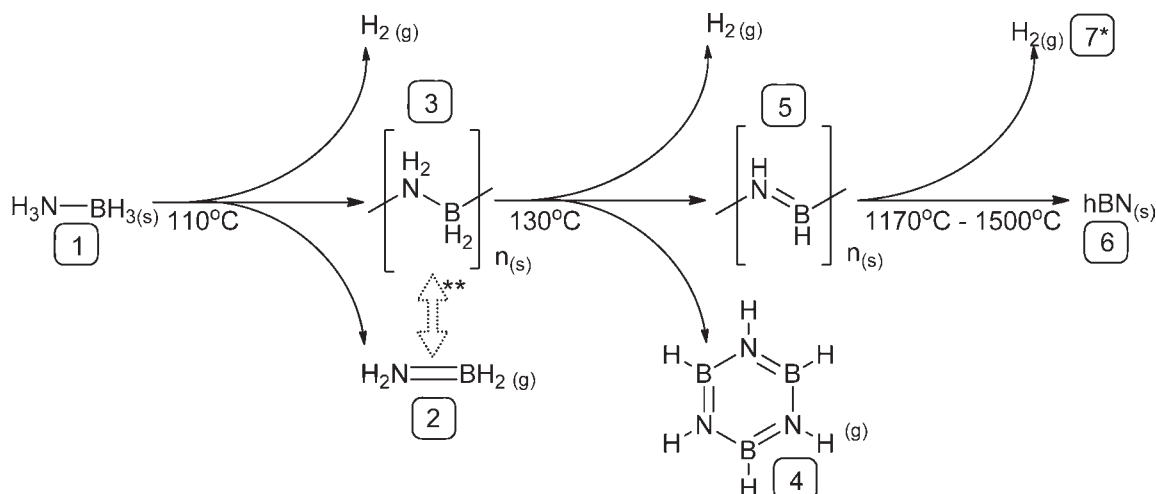
Other than the NH, BH, and BN stretching vibrations in this material, the remaining IR spectrum should be highly dependent on cis–trans isomerism, structural conformation, crystallinity, exact stoichiometry, degree of branching, and degree of cyclization in the polymer.<sup>12</sup> Unequivocal assignments to the remaining absorptions in this spectrum can not be made at this time because the effect of these multiple variables has not been well established.

**ATR-FTIR: AB-1500 °C.** The strong peak in AB-1500 °C at 1344 cm<sup>-1</sup> and the sharp transition at 790 cm<sup>-1</sup> are respectively coincident with IR active stretching and out of plane bending vibrations in hexagonal phase boron nitride.<sup>24,25</sup> [Figure 7d] The absence of NH and BH stretching peaks in this spectrum suggests that the hydrogen has been removed from the system by treatment at 1500 °C under nitrogen for 24 h.

**ATR-FTIR: Commercially Supplied hBN.** There are no active modes in the NH and BH stretching regions in the hBN spectra. There are a number of factors that could contribute to the different IR spectrum of AB-1500 °C and hBN at low wave numbers, namely, differences in crystallinity and the anisotropy of pure phase hBN. Infrared reflectance studies using linearly polarized light have determined that the direction of the polarization vector with respect to the  $c$  axis of the crystal affects absorbance frequency positions in hBN by over 100 cm<sup>-1</sup> because of the splitting of transverse and longitudinal optical phonons.<sup>25,26</sup> The spectrum of a powder using non-polarized light is therefore complicated. The complicating

(21) Dillen, J.; Verhoeven, P. J. *Phys. Chem. A* **2003**, *107*, 2570–2577.(22) Jacquemin, D. *J. Phys. Chem. A* **2004**, *108*, 9260–9266.(23) Bokkeker, K. W.; Shore, S. G.; Bunting, R. K. *J. Am. Chem. Soc.* **1966**, *88*, 4396–4401.(24) Hoffman, D. M.; Doll, G. L.; Eklund, P. C. *Phys. Rev. B* **1984**, *30*, 6051–6055.(25) Geick, R.; Perry, C. H. *Phys. Rev.* **1966**, *146*, 543–547.(26) Cai, Y.; Zhang, L.; Zeng, Q.; Cheng, L.; Xu, Y. *Solid State Commun.* **2007**, *141*, 262–266.



**Scheme 1.** Experimentally Observed Chemical Pathways in the Pyrolytic Decomposition of Ammonia Borane to Boron Nitride

Species found to be involved in ammonia borane pyrolysis: [1] Ammonia Borane; [2] Molecular Aminoborane; [3] Polyaminoborane (PAB); [4] Borazine; [5] Polyiminoborane (PIB); [6] Semi-Crystalline *P63/mmc* (hexagonal) boron nitride; [7\*] Hydrogen abstraction by the evolution of molecular hydrogen at high temperature, is assumed, but other possible pathways exist. \*\*Reversibility between molecular aminoborane, [2], and PAB, [3] is inferred and likely to depend on temperature, chain length, and the extent of branching in the PAB polymer. At low temperatures, PAB is preferred and at higher temperatures PAB decomposes into molecular aminoborane [2] hydrogen, borazine [4], and polyiminoborane [5].

effect of anisotropy would be diminished in a material of low crystallinity. Lattice vibrations are expected to be more pronounced in a highly crystalline material.

**XRD, SEM, and SAM Spectra: AB-1500 °C.** Powder XRD and SEM data identify differences in crystallinity between AB-1500 °C and the commercially supplied hBN. The powder diffraction pattern of AB-1500 °C contains weak and broad reflections which coincide in position and relative intensity with reflections from a crystalline, *P63/mmc* hexagonal phase boron nitride. *P63/mmc* hBN has a graphitic structure where N atoms are stacked in-line between the B atoms of adjacent sheets, and vice versa. This stacking pattern was identified by Pease<sup>27–29</sup> in 1952. The smallest discrete particles in AB-1500 °C are about 1 μm, but most are larger than 5 μm. The XRD pattern of AB-1500 °C is similar to what has been termed turbostratic boron nitride (tBN).<sup>30</sup> tBN is a specific type of defected hBN, where graphitic layers are stacked nearly parallel, but with random translational and rotational orientation. Highly crystalline samples of hBN cannot typically be obtained without annealing at 1600 °C–1800 °C or using seeding effects. Other researchers have prepared tBN and hBN from compounds similar to ammonia borane, PAB and PIB.<sup>12,31–33</sup>

Normalized peak intensities from SAM spectra of AB-1500 °C provide a measure of atomic composition by

comparison with normalized peak intensities from SAM spectra of hBN powder. The commercially supplied hBN has a sharp, tightly indexed diffraction pattern, and the material can be taken as stoichiometric. The AB-1500 °C and hBN samples have very similar nitrogen to boron peak intensity ratios [Table 1]. The instrument has a slightly different sensitivity to Auger electrons from each element so the peak intensity ratios are not expected to be 1:1. The carbon present on the surface of each sample is assumed to be adventitious. AB-1500 °C is therefore composed of nitrogen and boron in a 1:1 ratio. A small amount of oxygen impurity is present. Spot 2 from the AB-1500 °C sample has a slightly increased nitrogen to boron ratio probably caused by carbon based impurities. On the basis of IR, XRD, and SAM data, the AB-1500 °C material can be characterized as a semicrystalline boron nitride, structurally approximating the *P63/mmc* hexagonal phase species but lacking significant long-range order.

Additionally, a second sample of ammonia borane was heated to 1500 °C under pure anhydrous ammonia. There was no significant change to the XRD pattern or ATR-FTIR spectrum in comparison to the AB-1500 °C sample prepared under a nitrogen carrier gas. Ammonia performs a nucleophilic removal of carbon, oxygen, halogens, and free boron impurities which may inhibit crystallization processes. The reason fully crystalline species were not obtained after 24 h at 1500 °C is therefore thermodynamic, or related to atomic scale disorder prior to the third decomposition step. Toury et al.<sup>32</sup> have documented a “precursor memory” effect in their explorations of hBN preceramic polymers. Polymers which adopt conformations and packing structures similar to hBN tend to yield ceramic char with greater crystallinity.

**Quantitative and Semi-Quantitative Assessments.** ATR-FTIR data suggests that at least 2 mol equivalents of H<sub>2</sub> can be released from ammonia borane by pyrolysis at temperatures up to 210 °C. However, only 10 wt % hydrogen was typically obtained in our vacuum line

(27) Ooi, N.; Rairkar, A.; Lindsley, L.; Adams, J. B. *J. Phys.: Condens. Matter* **2006**, *18*, 97–115.

(28) Pease, R. *Acta Crystallogr.* **1952**, *5*, 356.

(29) Coleburn, N.; et al. *J. Chem. Phys.* **1968**, *48*, 555.

(30) Thomas, J.; Weston, N. E.; O’Conner, T. E. *J. Am. Chem. Soc.* **1963**, *84*, 4619.

(31) Wideman, T.; Remsen, E. E.; Cortez, E.; Chlanda, V. L.; Sneddon, L. G. *Chem. Mater.* **1998**, *10*, 412–421.

(32) Toury, B.; Duriez, C.; Cornu, D.; Miele, P.; Vincent, C.; Vaultier, M.; Bonnetot, B. *J. Solid State Chem.* **2000**, *154*, 137–140.

(33) Lebedev, B. V.; Kulagina, T. G. *J. Chem. Thermodyn.* **1991**, *23*, 1097–1106.

measurements, corresponding to 1.61 mol equivalents of  $H_2$ . An important reason for this discrepancy is the white coating which formed on the tubing walls between the liquid nitrogen trap and the sample and evolved hydrogen on gentle heating with a Bunsen burner. Similar condensed species were found at the exit of the furnace in TPD-MS experiments, as discussed previously. The triple point temperature of borazine is 215.6 °C, and borazine is a liquid at room temperature and atmospheric pressure.<sup>33</sup> Therefore, the coatings cannot be solid phase borazine. Physically and chemically condensed low molecular weight volatiles with an  $NBH_x$  stoichiometry where  $x \geq 2$  must be major constituents in these coatings because hydrogen is not readily evolved from  $\pi$  bonded nitrogen and boron atoms. The practical implications of these data are that reactor design could markedly influence hydrogen yield and hydrogen purity by controlling the amount of partially decomposed volatiles allowed to escape to cool areas.

**Chemical Pathways.** The pyrolytic decomposition pathways of ammonia borane that can be identified from this analysis are outlined in Scheme 1. This scheme corroborates the results of other researchers, (namely, Wolf et al. and Hess et al.) and includes the two major additions addressed below:

- (1) Molecular aminoborane evolves as a pyrolysis product concurrently with the evolution of hydrogen at about 110 °C. A reversible condition between molecular aminoborane and PAB is inferred. At 110 °C and above, the decomposition of PAB into molecular aminoborane is competitive with the formation of PIB and hydrogen. At room temperature, the polymeric form of molecular aminoborane is strongly preferred, and hydrogen evolving reactions do not occur. Chain length, degree of branching, and cyclization of the polymer should affect the rate of molecular aminoborane formation.
- (2) Hydrogen is abstracted from the solid phase residue beginning at 1170 °C, resulting in a semicrystalline *P63/mmc* (hexagonal) phase boron nitride after treatment at 1500 °C for 24 h in nitrogen and anhydrous ammonia. The concurrent evolution of molecular hydrogen is assumed.

Borazine and molecular aminoborane are unacceptable impurities in a fuel cell hydrogen stream. Neither mechanism of formation is precisely known. Baitalov et al.<sup>2</sup> have proposed that desorbed molecular  $NH_2= BH_2$  above 130 °C undergoes dehydrogenation to form a reactive

$HN\equiv BH$  (iminoborane) intermediate that rapidly trimerizes to form borazine. We are not aware of any physical evidence documenting the direct thermal conversion of molecular aminoborane to hydrogen and borazine. Another possibility is the direct evolution of iminoborane from the condensed phase pyrolysis residue after PIB structures begin to form above 130 °C, followed by rapid trimerization. The evolution and rapid association of diborane and ammonia to form borazine and hydrogen gas is unlikely.<sup>15</sup>

## Conclusions

Taken together, the TGA, DSC, TPD-MS, vacuum line, XRD, SAM, and ATR-FTIR data suggest hydrogen is lost from ammonia borane in three major stages in roughly equal amounts. Ammonia borane first decomposes into a material structurally approximating PAB, then PIB. The evolution of partially decomposed volatiles can affect the amount of hydrogen evolved during the first two decomposition steps. Subsequent higher temperature processes starting at 1170 °C lead to the formation of a semicrystalline hexagonal, *P63/mmc*, graphite phase, boron nitride. These pathways are shown in Scheme 1. Trace amounts of  $H_2O$  and  $O_2$  can markedly influence the decomposition process, and reactor configuration can potentially have a significant effect on hydrogen yield. Infrared vibrational spectra of thermally treated ammonia borane, at known temperatures, have provided information regarding pathways of decomposition.

**Acknowledgment.** We acknowledge Justin Reutenauer, and Will Osborn for experimental assistance. The research reported in this document was performed under prime contracts W909MY-06-0041 and W15P7T-07-C-P420 through Ensign-Bickford Aerospace & Defense Company with U.S. Army CECOM ACQ Center. The views and conclusions contained in this document are those of the authors, and should not be interpreted of the U.S. Government unless so designated by other authorized documents. Citation of manufacturers or trade names created as presenting the official policies or position, whether expressed or implied, of the U.S. Army CECOM, ACQ Ceoes not constitute an official endorsement or approval of the use thereof. The U.S. Government is authorized to reproduce and distribute reprints for Government purposes notwithstanding any copyright notation hereon. Some characterization was done with the support of the Department of Energy, Office of Basic Energy Sciences, Division of Chemical, Geochemical, and Biological Sciences.